J. Fluid Mech. (1979), *vol.* 90, *part* 2, *pp.* 227–239
Printed in Great Britain

An experimental investigation of natural convection in the melted region around a heated horizontal cylinder

By A. G. BATHELT, R. VISKANTA AND W. LEIDENFROST

Heat Transfer Laboratory, School of Mechanical Engineering, Purdue University, West Lafayette, Indiana 47907

(Received 21 December 1977)

Melting from an electrically heated horizontal cylinder embedded in a paraffin (*n*-octadecane, fusion temperature 301·3 °K) has been studied experimentally. The shape of the solid-liquid interface has been determined photographically, and the local heat transfer coefficients have been measured using a shadowgraph technique. The experiments provide conclusive evidence of the important role played by natural convection in melting a solid due to an embedded cylindrical heat source. The four distinct pieces of quantitative evidence which contribute to this conclusion are the melt shape, surface temperature, local and average heat transfer coefficients and their variation with time.

The experimental findings prove the importance of natural convection in phase change problems involving melting and indicate that continued practice of neglecting the effects in the analysis of such problems does not appear reasonable. Natural convection should be considered in analysis and design of systems involving phase change.

1. Introduction

Phase change heat transfer such as melting and freezing is not only of interest in a wide range of technologies but also in geophysics. Problems of this type are important in crystal growth from melts and solutions, purification of materials, solidification of castings, freeze drying of foodstuffs, thermal control of spacecraft using phase change materials, melting of ice and freezing of waters, thermal energy storage and many others. Temperature variations in the liquid are of necessity present during heat transfer, and these temperature differences may be sufficiently large to generate buoyancy forces for unstable situations which could produce natural convection motions. The convection in the liquid could have an important bearing on the motion of the phase change boundary and heat transfer.

Aside from the studies of convective instabilities in the melting of horizontal ice layers (Martin & Kauffman 1974; Seki, Fukusako & Sugawara 1977) experiments do not appear to have been reported which specifically address this problem. Recent experiments (White *et al.* 1977; Sparrow, Schmidt & Ramsey 1978; Bathelt, Viskanta & Leidenfrost 1978) have provided conclusive evidence that natural convection plays an important role in the melting of a solid surrounding an embedded horizontal heat source. Theoretical considerations of the possible role of natural convection in the melt region during heat transfer with phase change have received practically no

attention (Bankoff 1964; Rubinstein 1971). Until recently, the effect of natural convection in the melting of a solid due to an embedded heat source has been neglected and heat transfer was assumed to be by pure conduction (Horsthemke & Marschall 1976; Shamsundar & Sparrow 1976). As a result, the solid–liquid interfaces formed are a succession of concentric circles surrounding a cylindrical heat source. Very recently an analysis of multi-dimensional melting from a vertical cylinder embedded in a solid which takes into account natural convection in the melt region has been performed (Sparrow, Patankar & Ramadhyani 1977). The findings of this study indicate that natural convection is of first-order importance and has to be considered in phase change analyses.

The preliminary results available (White *et al.* 1977) show that natural convection affects the circumferential variation of the local heat transfer coefficient, the variation with time of the local and average coefficients and the shape of the solid–liquid interface. For example, as natural convection develops in the melt the melting front becomes asymmetrical about a heated horizontal cylinder embedded in a solid. A plume formed above the heat source conveyed the hot liquid to the upper portion of the melt region and supported the upward movement of the interface. As a result of this upward thrust of the melting zone the primary melting took place above the cylinder.

The experiments (Sparrow *et al.* 1978) published subsequent to the submission of this paper appear to be concurrent and independent efforts. The experiments were performed with a eutectic mixture of sodium nitrate and sodium hydroxide, which has a melting temperature of about 244 °C. Only spatial averaged (over the surface of an electrically heated, horizontal cylinder) heat transfer coefficients and the melting front positions determined from thermocouple readings are reported. Qualitative findings are mutually supportive. Quantitative comparison cannot be made because of the different materials employed and because the transport properties of the salt eutectic do not appear to be available.

Natural convection is an important process in problems involving melting/freezing, and it is the purpose of this paper to point out some of its characteristics. To this end, heat transfer processes which occur when a solid is melted by a heat source embedded within the solid are studied. Quantitative experimental evidence is presented on the role of natural convection in the melt region in the motion of the phase change boundary and the heat transfer coefficients when a horizontal cylinder embedded in *n*-octadecane was heated electrically. The paraffin was chosen as a test material because the liquid is transparent, allowing for optical and photographic observation of the melt zone, and because paraffins have been suggested (Lorsch *et al.* 1975) as phase-change-materials (PCM) for thermal energy storage systems taking advantage of the latent heat of fusion of the storage medium. Another reason for using a paraffin, such as *n*-octadecane, is that its properties are well established (Smith 1936; Doss 1943; Maxwell 1950; Egloff 1953; Kurtz & Sankin 1953; Dreisbach 1959) and thus facilitate the proper non-dimensionalization which is necessary in generalizing the results. In addition, *n*-octadecane has a fusion temperature of 301·3 °K which is conducive for reducing the heat losses from the test cell to the ambient laboratory environment.

The results of the melting experiments provide evidence about the melting front and its change with time, and give immediate insight into the nature of the transport processes in the melt region. The evidence furnished on the role of natural convection

in the melt zone on the heat transfer is in the form of solid–liquid interface position, local heat transfer coefficients and the average heat transfer coefficient variation with time.

2. Experiments

Test apparatus and test procedure

To model the energy storage cell, a rectangular test cell (162 × 132 × 40 mm), in which melting and solidification occur essentially in two directions, was designed and built. Front and back sides of the cell were made of plate glass, 6 mm thick, to allow visualization, photographing and optical observation of the phenomena taking place during phase transformation. To reduce free convection from the outside of the cell, a double window was used with a gap of 12 mm between the two vertical glass plates. The spacing between the plates was so selected as to prevent free convection in the enclosed air gap.

An electrical cartridge heater, 0·64 cm outside diameter, was employed as a heating element. The heater was inserted in a snugly fitting copper tube, 1·9 cm in outside diameter. The 4·0 cm long tube with the heater inside was then installed in the test cell. A hole was drilled in the glass plate for inserting the heater unit and bringing out the power leads. The hole was then sealed to prevent the molten paraffin from leaking from the cell. The electrical power to the heater element was supplied by a variable transformer and monitored on a wattmeter.

The wall temperatures were measured by chromel–constantan thermocouples. Small diameter, 1·0 mm O.D., holes were drilled axially in the copper tube and then brought to the surface, soldered and the surface polished. The thermocouples were located at $\theta = 0^\circ, 90^\circ, 180^\circ$ and 270°. A shadowgraph system, shown schematically in figure 1, was employed for observing the melting front and for measuring the local heat transfer coefficient at the surface of the cylinder (Hauf & Grigull 1970). The system has been found to be satisfactory in preliminary experiments (White *et al.* 1977).

The test cell was filled with liquid *n*-octadecane (99 % pure, Humphrey Chemical Co., North Haven, CT) and given sufficient time to solidify and reach uniform ambient temperature throughout. The initial temperature of the solid was maintained close to the melting temperature and was typically a maximum of only a couple of degrees Kelvin lower than the melting temperature. Therefore, the small subcooling $(T_f - T_i)$ (fusion temperature–initial temperature) is not expected to have much effect on the melting front motion. Each experiment was performed at constant electrical power input (constant heat flux) to the heater. The maximum beam deflexion and the motion of the melting front were recorded photographically.

Data reduction

If a parallel light beam enters a uniform test-section it remains so toward the screen. During the melting process, however, the material in the test section is non-uniform owing to temperature gradients which cause a change of index of refraction of the PCM. Since the light beam remains deflected outside of the test cell, the displacement on the screen can be minimized by moving the screen as close as possible to the exit of the test section in contrast to studying heat transfer around the heat source where a large

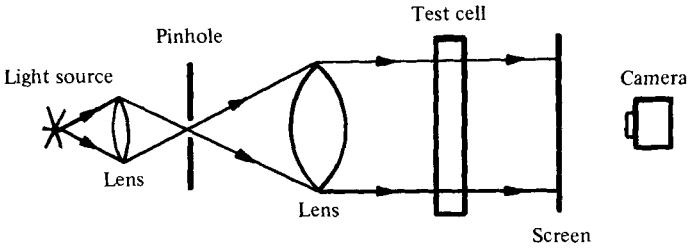

FIGURE 1. Schematic diagram of the optical system.

displacement is necessary for a quantitative evaluation of the photographs. In that case, a sufficient distance l between test section and screen has to be maintained.

The path of light in a non-isothermal medium can be calculated from the geometrical optics theory (Hauf & Grigull 1970). For a system where changes in the index of refraction n and of the temperature in the axial direction are negligible in comparison with the radial direction, the geometrical optics theory yields the distance Y of the deflected light beam on the screen

$$Y = \frac{1}{n}\frac{dn}{dT}\frac{dT_l}{dr} lL, \tag{1}$$

where T_l is temperature of liquid, r is radial distance and L is length of cylinder.

For a horizontal cylinder of radius R the local Nusselt number Nu defined by

$$Nu = -\frac{2(\partial T_l/\partial r)_R R}{(T_w - T_f)} \tag{2}$$

can be expressed in terms of observed and known quantities as

$$Nu = -n\frac{dT}{dn}\frac{2RY}{lL(T_w - T_f)}, \tag{3}$$

where T_w is the cylinder surface temperature. The distance Y is determined from the photographs made during the melting process. A more detailed discussion of the theoretical basis of the shadowgraph technique is given elsewhere (Schmidt 1932; Schmidt & Leidenfrost 1953; Hauf & Grigull 1970).

3. Results and discussion

Melt shape

The photographs presented in figure 2 (plate 1) illustrate the positions of the solid–liquid interface at selected times for two different wall heat fluxes. The contours of the cylinders are indicated with a dashed line. The shadows of the cylinders appear to be slightly greater and out of round. This is not due to faulty imaging but to the fact that the photographs of the melt shapes were made off the screen attached to the test cell instead of photographing the cylinder directly.

At early times ($\tau = 0{\cdot}96$, τ is dimensionless time (Fourier number), $\tau = kt/R^2\rho c$) when heat transfer in the melt zone is predominantly by conduction, the molten region is symmetrical about the axis of the cylinder. From the study of the shadowgraphs and the melt shapes, the time τ, the wall temperature T_w and the gap width δ

Ste	τ	$\frac{T_w - T_f}{qR/k}$	$\delta/2R$	Gr_δ
0·587	1·92	0·127	0·269	1590
0·881	0·96	0·110	0·218	1090
1·175	0·58	0·101	0·192	917

TABLE 1. Parameters at the first occurrence of instability.

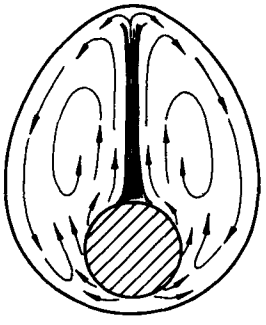

FIGURE 3. Circulation pattern for a vertically oriented plume.

at which instability was first observed are given in table 1. At these times the melting fronts were still symmetrical about the cylinder axis. The Grashof number is based on the gap width δ to correspond with the definition used by Grigull & Hauf (1966) in their study of natural convention in an annulus. The Grashof numbers in the table are in what has been referred to as the 'two-dimensional pseudo-conductive regime'. According to the stability criteria developed by Vest & Lawson (1972) for natural convection from a horizontal wire in an unbounded fluid, the delay time for $Ste = 1{\cdot}175$ (Stefan number, $Ste = cqR/k\Delta h_l$) at which significant convection is initiated was estimated to be about 8 seconds, while the observed time was about 12 minutes. A direct comparison of the two results is not appropriate since Vest & Lawson based their critical Rayleigh number on the Bénard problem with rigid lower and free upper boundaries. During the early phase of heating in the present experiments the liquid is confined between the rigid heated cylinder and a concentric, moving solid–liquid interface. Therefore, the geometry of this problem corresponds more closely to that of Grigull & Hauf (1966) than that of Vest & Lawson (1972).

Even at early times a plume is already developed at the top of the cylinder and can be clearly seen in figure 2(*b*) at $\tau = 0{\cdot}96$. The plume conveys hot liquid to the upper part of the melt region, which is indicated schematically in figure 3, and continues to support the upward movement of the interface. The circulation pattern sketched in figure 3 was observed visually by following the motion of very small (less than 0·1 mm size) paraffin particles which were present in the melt. Since the *n*-octadecane was only 99 % pure it is suspected that these particles were paraffins with a higher molecular weight having a higher melting temperature. The oscillation of the plume above the cylinder is evident from the photographs, but observations revealed no definite period of plume oscillations. The symmetrical circulation pattern indicated in the figure occurs only when the plume originates at the top of the cylinder and not when it is

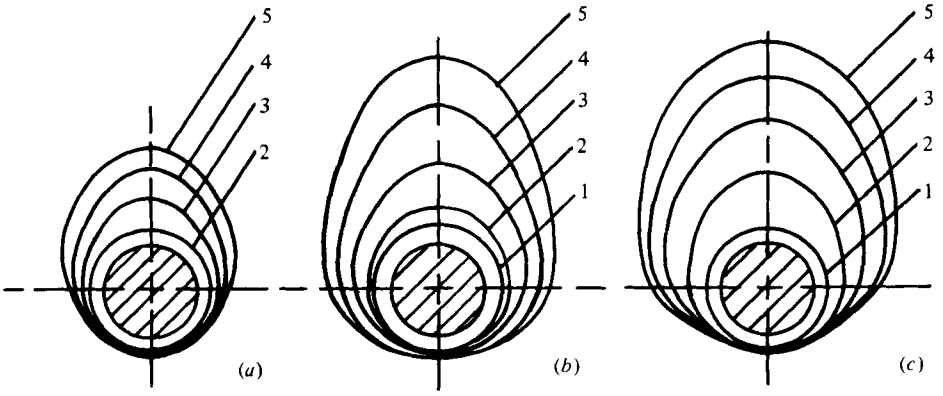

FIGURE 4. Experimentally determined melt contours at different times (1, $\tau = 0{\cdot}96$; 2, $\tau = 1{\cdot}92$; 3, $\tau = 3{\cdot}84$; 4, $\tau = 5{\cdot}76$; 5, $\tau = 7{\cdot}68$): (*a*) $Ste = 0{\cdot}587$, (*b*) $Ste = 0{\cdot}881$ and (*c*) $Ste = 1{\cdot}175$.

off to a side as seen in figure 2(*b*). As the heating continues and natural convection develops, the molten annular region becomes increasingly distorted and takes on a 'pear-like' shape, i.e. (*a*) $\tau = 3{\cdot}84$, and (*b*) $\tau = 1{\cdot}92$.

In figures 4(*a*)–(*c*) the positions of the solid–liquid interface at a succession of times are plotted for three different Stefan numbers (heat fluxes) of 0·587, 0·881 and 1·175, respectively. The melting front positions were taken directly from the photographs. Inspection of the figures reveals that at early times or low heat fluxes at all times the melt regions are similar in shape and that when heat transfer to the paraffin is predominantly by conduction the melt region is symmetrical about the axis of the cylinder. At longer times, after natural convection had developed, the molten annular zone becomes increasingly distorted.

The shapes of the melt zone shown in figure 4 for *n*-octadecane are different for the same surface heat flux than those for SUNOCO P-116 wax (White *et al.* 1977). The molten region was somewhat more slender and sharper near the top for P-116 wax than *n*-octadecane. Greater heat loss from the test cell wall and larger initial subcooling of the solid for SUNOCO P-116 wax are considered to be the main reasons for the differences. The parameter $c_s(T_f - T_i)/\Delta h_l$ can be used as a measure of the importance of initial subcooling on the shape of the melt zone, c_s is specific heat of the solid and Δh_l is latent heat of fusion. For *n*-octadecane this parameter was a maximum of 0·03 while for SUNOCO P-116 it was 0·4. This clearly indicates that very little energy was required to bring *n*-octadecane to the fusion temperature as compared with the latent heat of fusion while a substantial fraction of heat input was needed for P-116 wax.

The results of figure 4 show that melting takes place primarily above the cylinder, with very little occurring below. The strong upward thrust of the melting zone is caused by natural convection. At early times a plume rises from the top of the heated cylinder, and at later times circulation conveys the hot liquid to the upper part of the melt zone and in this manner continues to support the upward movement of the solid–liquid interface. As the Stefan number increases the solid above the cylinder melts faster and affects the overall shape of the molten zone. A direct comparison of the melt shapes determined in this work and those reported in the literature (Sparrow *et al.* 1978) is not possible because of different materials and thermal conditions used. Qualitatively, the melt shapes are similar.

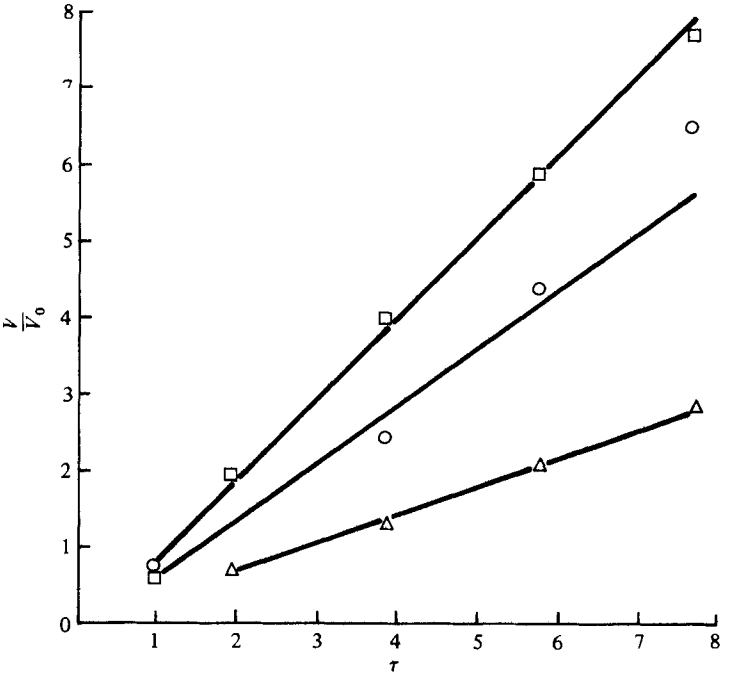

FIGURE 5. Variation of dimensionless (V_0 = volume of the heat source) melt volume with time. □, $Ste = 1{\cdot}175$, $T_i = 296$ °K; ○, $Ste = 0{\cdot}881$, $T_i = 299{\cdot}5$ °K; △, $Ste = 0{\cdot}587$; $T_i = 298$ °K.

From the results given in figure 4, the volume and mass of the material melted can be determined as a function of time. The data presented in figure 5 show that for $\tau > 1{\cdot}0$, the melt volume increases almost linearly with time. This was expected as the subcooling was very small and the constant heat input at the cylinder wall was almost entirely used to melt the *n*-octadecane. At early times the volume of the melt is small and difficult to determine accurately and for this reason is not given. During the initial phase of melting heat transfer is by conduction and the overall process is not one of quasi-steady nature. The first indication of natural convection was observed at $\tau \simeq 0{\cdot}58$ for $Ste = 1{\cdot}175$.

Cylinder surface temperature

The cylinder surface temperature (at $\theta = 180°$) time history measured with a thermocouple is shown in figure 6. There was relatively small variation in the surface temperature along the cylinder, but there was some variation of T_w with the angular position θ. The maximum surface temperature typically occurred at $\theta = 180°$, but the maximum difference never exceeded 0·5 °K for the largest wall heat flux,

$$q = 1671\,\mathrm{W/m^2}; \quad Ste = 1{\cdot}175.$$

At $Ste = 1{\cdot}175$ and $Ste = 0{\cdot}881$ distinct 'overshoots' in the wall temperature were noted at $t = 15$ and $t = 20$ minutes, respectively. Similar type of overshoots have been observed in transient natural convection heat transfer from a vertical plate (Goldstein & Eckert 1960) and expected for transient heating of a cylinder immersed in a liquid (Fand & Keswani 1973). After some time the surface temperature approached a

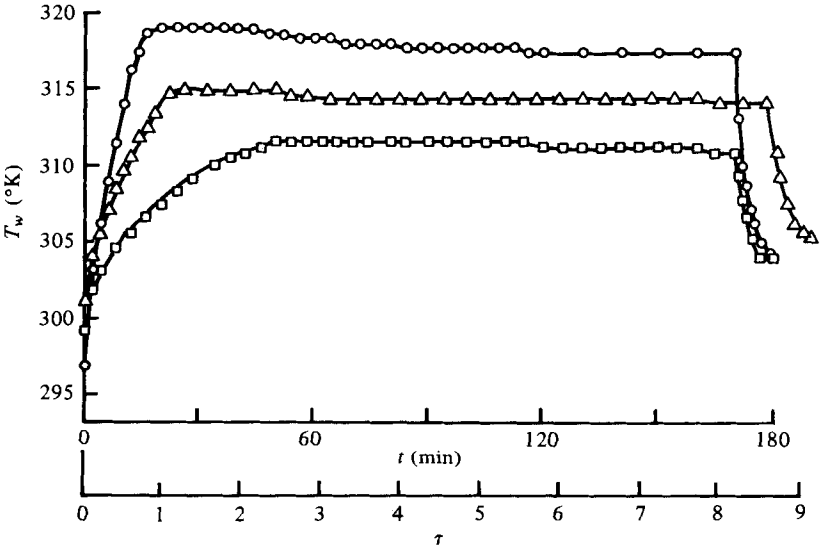

FIGURE 6. Variation of surface temperature of the heated cylinder with time. ○, $Ste = 1{\cdot}175$; △, $Ste = 0{\cdot}881$; □, $Ste = 0{\cdot}587$.

constant value. The surface temperature decreased very sharply after the power to the cylinder was shut off.

The study of the shadowgraphs revealed that the first indication of instability (see table 1) occurred shortly before the cylinder surface reached its maximum temperature. The occurrence of the peak surface temperature is considered to be associated with the change from pseudo-conduction through transition to the fully developed natural convection regime. The smoke studies and interference pictures of Grigull & Hauf (1966) in the transition regime (between pseudo-conduction and fully developed natural convection) indicate an onset of change in the flow pattern in the form of three-dimensional vortices of an unsteady oscillating kind. In the fully developed natural convection regime the motion returns to two-dimensional form. The shadowgraph pictures shown in figure 7 (plate 2) also appear to indicate the growth of longitudinal vortices, a process which is expected to follow a thermal instability at the top. In brief, the overshoot is considered to be associated with the change of flow motion in the gap between the cylinder and the solid–liquid interface.

The average heat transfer coefficient (averaged over the circumference and length of the cylinder) for a constant heat input to the cylinder is inversely proportional to $\bar{T}_w - T_f$ (average surface temperature $\bar{T}_w$ minus fusion temperature T_f) and the results of figure 6 give immediate insight into the average heat transfer coefficient ($\bar{h}$) variation with time,

$$\bar{h} = \frac{q}{(\bar{T}_w - T_f)}. \tag{4}$$

However, since the heat losses from the end of the cylinder to the test cell wall could not be estimated very accurately this method of determining the average heat transfer coefficient was not used.

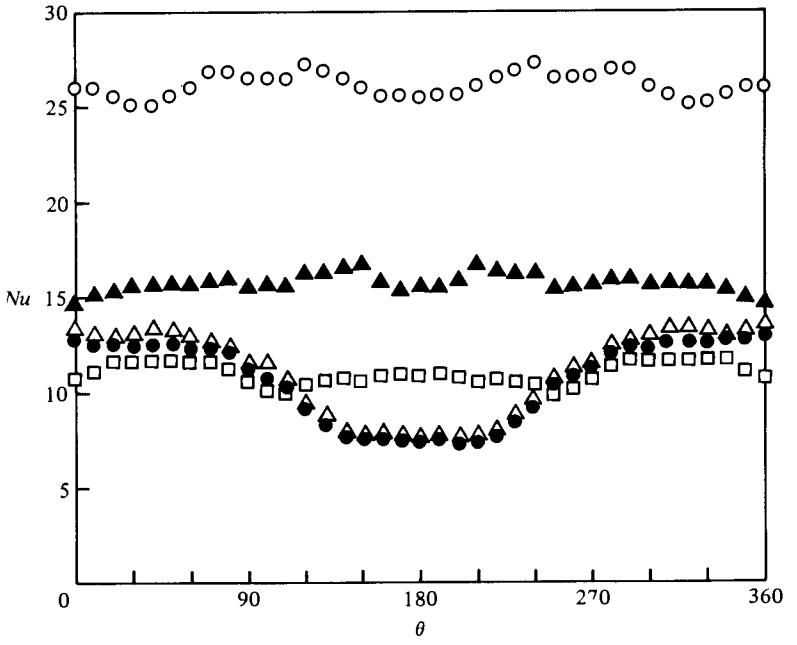

FIGURE 8. Variation of local Nusselt number around the cylinder for *Ste* = 0·587. ○, τ = 1·056; ▲, τ = 1·44; □, τ = 1·92; ●, τ = 3·072; △, τ = 3·84.

Heat transfer

Two shadowgraphs of a heated cylinder during the melting process are shown in figure 7. The dynamic process of developing natural convection is clearly evident from the still photographs for *Ste* = 0·587. The beginning of natural convection can be seen from figure 7(*a*). The regular cells formed on the upper part of the cylinder at τ = 1·92 are indicative of laminar convection (Grigull & Hauf 1966). As the heating continued the cells increased in size (τ = 2·11) and completely disappeared at τ = 2·21.

The local Nusselt number can be deduced from the shadowgraphs. Since the light beams grazing the cylinder surface are deflected the most, they form the light zone around the dark shadow in the centre. The distance on the screen from the cylinder surface, indicated by the slashed circle, to the light/dark boundary is directly proportional to the temperature gradient at the cylinder surface ($r = R$), and therefore to the local Nusselt number.

The local Nusselt numbers determined from (3) are plotted in figures 8, 9, and 10 for Stefan numbers 0·587, 0·881 and 1·175, respectively. Before discussing the results it should be emphasized that the nature of the shadowgraph technique allows determination of only the average surface temperature gradient, $(dT/dr)_{r=R}$, over the entire length of the heated cylinder, see (1). Therefore, any non-uniformities in the gradient along the cylinder axis as a result of heat losses from the ends of the cylinder to the test cell walls are accounted for, and the Nusselt numbers given in the figures should be considered as averaged values over the cylinder length. Results are not given in figures 9 and 10 in the immediate vicinity of the upper stagnation point ($\theta \approx 180°$) because of the experimental difficulties of accurately determining Y in this region from the photographs.

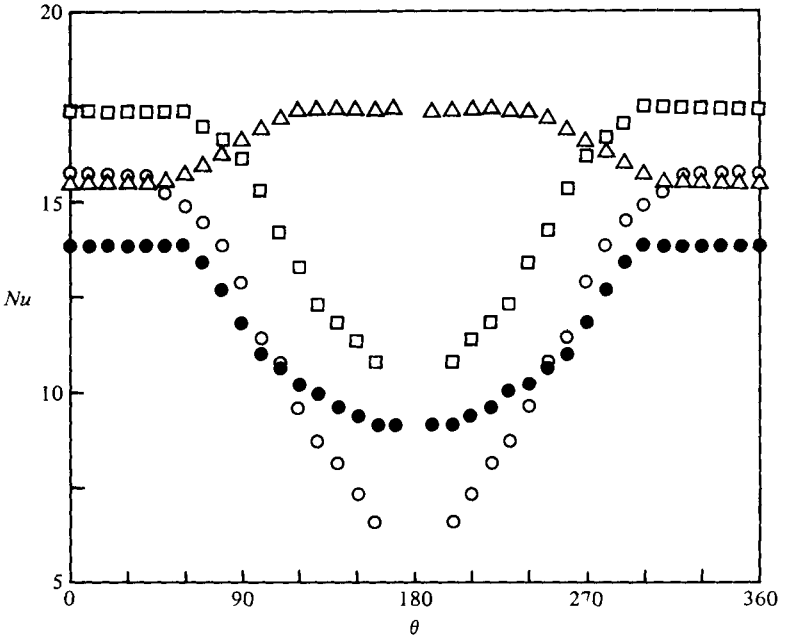

FIGURE 9. Variation of local Nusselt number around the cylinder for $Ste = 0{\cdot}881$. △, $\tau = 0{\cdot}672$; ●, $\tau = 1{\cdot}248$; ○, $\tau = 1{\cdot}92$; □, $\tau = 2{\cdot}88$.

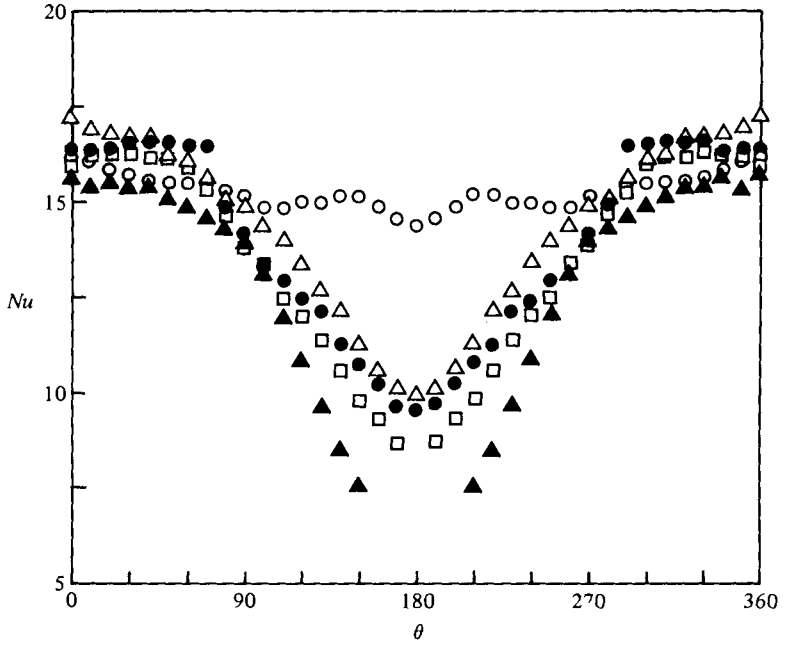

FIGURE 10. Variation of local Nusselt number around the cylinder for $Ste = 1{\cdot}175$. ○, $\tau = 0{\cdot}53$; △, $\tau = 0{\cdot}96$; □, $\tau = 1{\cdot}92$; ●, $\tau = 2{\cdot}88$; △, $\tau = 3{\cdot}84$.

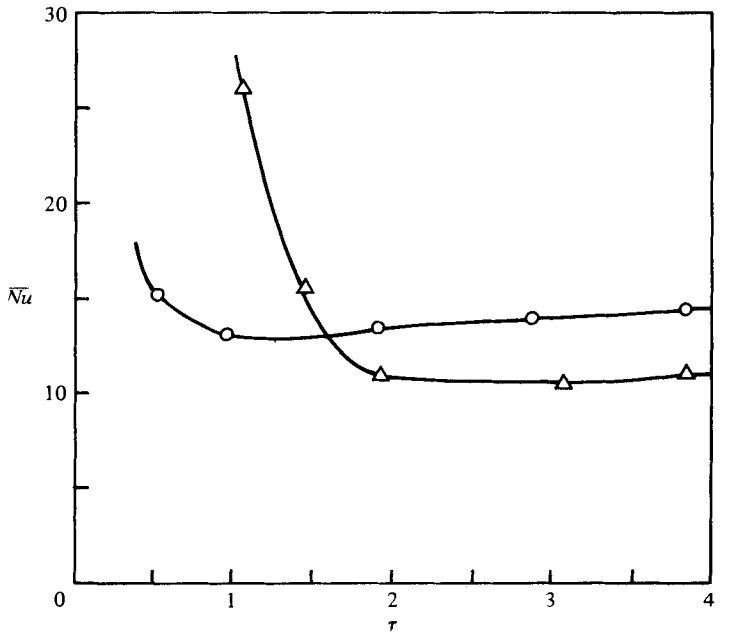

FIGURE 11. Variation of the average Nusselt number with time. ○, $Ste = 1{\cdot}175$, △, $Ste = 0{\cdot}587$.

At early times, $\tau = 1{\cdot}056$ in figure 8 and $\tau = 0{\cdot}672$ in figure 9, conduction is the dominant mechanism of heat transfer, and the local Nusselt numbers are characteristic of that phase. During this phase the heat transfer coefficient decreases monotonically with time and is practically independent of the angular position around the cylinder. As the melting continues and natural convection develops the Nusselt number becomes more non-uniform. Inspection of the figures reveals that Nu is almost independent of the angular position in about the lower third of the cylinder ($0 \leqslant \theta < 60°$ and $300° < \theta \leqslant 360°$) and is most non-uniform in the upper two thirds ($60° < \theta < 300°$). Comparison of the results presented in figures 8 and 10 show, for example, that the variation of the local Nusselt number is greater for the larger Stefan number. This is primarily because at a given time natural convection is more intense for the larger Stefan number as a result of a greater melt zone.

Examination of the results presented in figures 8, 9 and 10 reveals complex trends in the local Nusselt number variation with time and angular position. This is because of the competing mechanisms of heat transfer by conduction and natural convection as well as the changing circulation patterns as a consequence of altered shape and size of the melt zone. For example, figure 10 demonstrates that the local Nusselt number in the upper two-thirds of the cylinder reaches a minimum with time.

The average heat transfer coefficient variation with time is presented in figure 11. Inspection of the figure reveals that the average Nusselt number ($\overline{Nu}$) decreases with time when heat transfer is by conduction. The Nusselt number reaches a constant steady-state value at large times even though the liquid–solid interface continues to move as melting progresses. This suggests that the processes which occur in the neighbourhood of the interface do not contribute significantly to the overall thermal resistance to heat transfer. The minimum in the Nusselt number corresponds to the

overshoot in the cylinder surface temperature which has already been discussed. The instantaneous (spatially averaged) heat transfer coefficients determined during melting of a salt eutectic (Sparrow *et al.* 1978) also showed a minimum. Because the wall heat fluxes in these experiments were higher than those reported in this paper the minimum is also more distinct. Since the cylinder was heated uniformly, it follows from the definition of $\bar{h}$ that an overshoot in the cylinder surface temperature also existed, but these data were not reported in the paper.

The onset of natural convection and attainment of the steady state (constant $\overline{Nu}$) occur at earlier times for the higher Stefan number. In addition, the higher the Stefan number, the larger are the Nusselt numbers. These trends appear to be reasonable inasmuch as higher Stefan numbers correspond to larger melt zones, higher cylinder surface temperatures and therefore higher values of the Grashof number. Even though the experimental methods for determining the average heat transfer coefficients and the material used in this study was different from that of Sparrow *et al.* (1978) the qualitative findings are mutually supportive. They have also reported attainment of steady-state heat transfer coefficients. The coefficients increased and the attainment of the steady state occurred at earlier times for the higher surface heat fluxes.

4. Conclusions

The results presented in the paper provide strong evidence of the important role played by natural convection in the melting of a solid due to an embedded cylindrical heat source. There are four distinct pieces of evidence which contribute to this conclusion. First, the positions of the solid–liquid interface showed that melting primarily occurred above the cylinder with very little melting below. Second, the variation with time of the cylinder surface temperature deviated markedly from that which would have been predicted from a pure conduction model and was characteristic of transient natural convection. Third, the variation with angular position and time of the local Nusselt number showed that the heat transfer coefficients deviated markedly from the monotonic decrease with time that is characteristic of conduction phase change with no angular variation. Fourth, the variation with time of the average Nusselt number indicated that conduction dominates only during the early stages of the melting process but that natural convection comes into play and ultimately gives rise to a steady value of the heat transfer coefficient.

The experimental investigation of natural convection during melting of a solid from an embedded heat source provides quantitative description of the physical processes which occur during the transition from pure conduction heat transfer at the onset of melting to fully developed natural convection. Then the processes can be considered as being nearly quasi-steady.

The work described in the paper was supported by the National Science Foundation Heat Transfer Program, under Grant No. ENG 75-15030.

REFERENCES

BANKOFF, S. G. 1964 Heat conduction and diffusion with a phase change. *Advances in Chemical Engineering* (ed. T. B. Drew *et al.*), vol. 5, pp. 75–150, Academic Press.

BATHELT, A. G., VISKANTA, R. & LEIDENFROST, W. 1978 Experiments on the role of natural convection and heat source arrangement in the melting of a solid. *A.S.M.E. Paper* 78-HT-47.

DOSS, M. P. 1943 *Physical Constants of the Principal Hydrocarbons*. The Texas Company.

DREISBACH, R. R. 1959 *Physical Properties of Chemical Compounds*. Advances in Chemistry Series, American Chemical Society, no. 22.

EGLOFF, G. 1953 *Physical Constants of Hydrocarbons*. American Chemical Society, Monograph Series.

FAND, R. M. & KESWANI, K. K. 1973 Mass rate of flow in the natural convection plume above a heated horizontal cylinder immersed in a liquid. *J. Heat Transfer* **95**, 192.

GOLDSTEIN, R. J. & ECKERT, E. R. G. 1960 The steady and transient free convection boundary layer on a uniformly heated vertical plate. *Int. J. Heat Mass Transfer* **1**, 208.

GRIGULL, U. & HAUF, W. 1966 Natural convection in horizontal annulii. *Proceedings of the 3rd International Heat Transfer Conference*, American Institute of Chemical Engineers, vol. 2, pp. 182–195.

HAUF, W. & GRIGULL, U. 1970 Optical methods in heat transfer. *Advances in Heat Transfer* (ed. J. P. Hartnett & T. F. Irvine), vol. 6, pp. 133–366. Academic Press.

HORSTHEMKE, A. & MARSCHALL, E. 1976 Speicherung von Thermischer Energie in Salz- und Metallschmelzen. *Brennstoff-Wärme-Kraft* **28** (1), 18.

KURTZ, S. S. & SANKIN, A. 1953 Density and refractive index of hydrocarbons. *Physical Chemistry of the Hydrocarbons* (ed. A. Farkas), vol. 2, pp. 1–80. Academic Press.

LORSCH, H. G., KAUFFMAN, K. W. & DENTON, J. C. 1975 Thermal energy storage for solar heating and off-peak air conditioning. *Energy Conversion* **15**, 1.

MARTIN, S. & KAUFFMAN, P. 1974 The evolution of under-ice melt ponds, or double diff usion at the freezing point *J. Fluid Mech.* **64**, 507.

MAXWELL, J. B. 1950 *Databook on Hydrocarbons*. Van Nostrand.

RUBINSTEIN, L. I. 1971 *The Stefan Problem*. Trans. Math. Monogr., American Mathematical Society.

SCHMIDT, E. 1932 Schlierenaufnahmen des Temperaturfeldes in der Nähe wärmeabgebender Körper. *Forschung* **3**, 181.

SCHMIDT, E. & LEIDENFROST, W. 1953 Der Einfluss electrischer Felder auf den Wärmetransport in flüssigen electrischen Nichtleitern. *Forsch. Ing. Wes.* **19**, 65.

SEKI, N., FUKUSAKO, S. & SUGAWARA, M. 1977 A criterion of onset of free convection in a horizontal melted water layer with free surface. *J. Heat Transfer* **99**, 92.

SHAMSUNDAR, N. & SPARROW, E. M. 1976 Effect of density change on multidimensional conduction phase change. *J. Heat Transfer* **98**, 550.

SMITH, J. F. D. 1936 The thermal conductivity of liquids. *Trans. A.S.M.E.* **58**, 719.

SPARROW, E. M., PATANKAR, S. V. & RAMADHYANI, S. 1977 Analysis of melting in the presence of natural convection in the melt region. *J. Heat Transfer* **99**, 520.

SPARROW, E. M., SCHMIDT, R. R. & RAMSEY, J. W. 1978 Experiments on the role of natural convection in the melting of solids. *J. Heat Transfer* **100**, 11.

VEST, C. M. & LAWSON, M. L. 1972 Onset of convection near a suddenly heated horizontal wire. *Int. J. Heat Mass Transfer* **15**, 1281.

WHITE, R. D., BATHELT, A. G., LEIDENFROST, W. & VISKANTA, R. 1977 Study of heat transfer and melting front from a cylinder imbedded in a phase change material. *A.S.M.E. Paper* 77-HT-42.

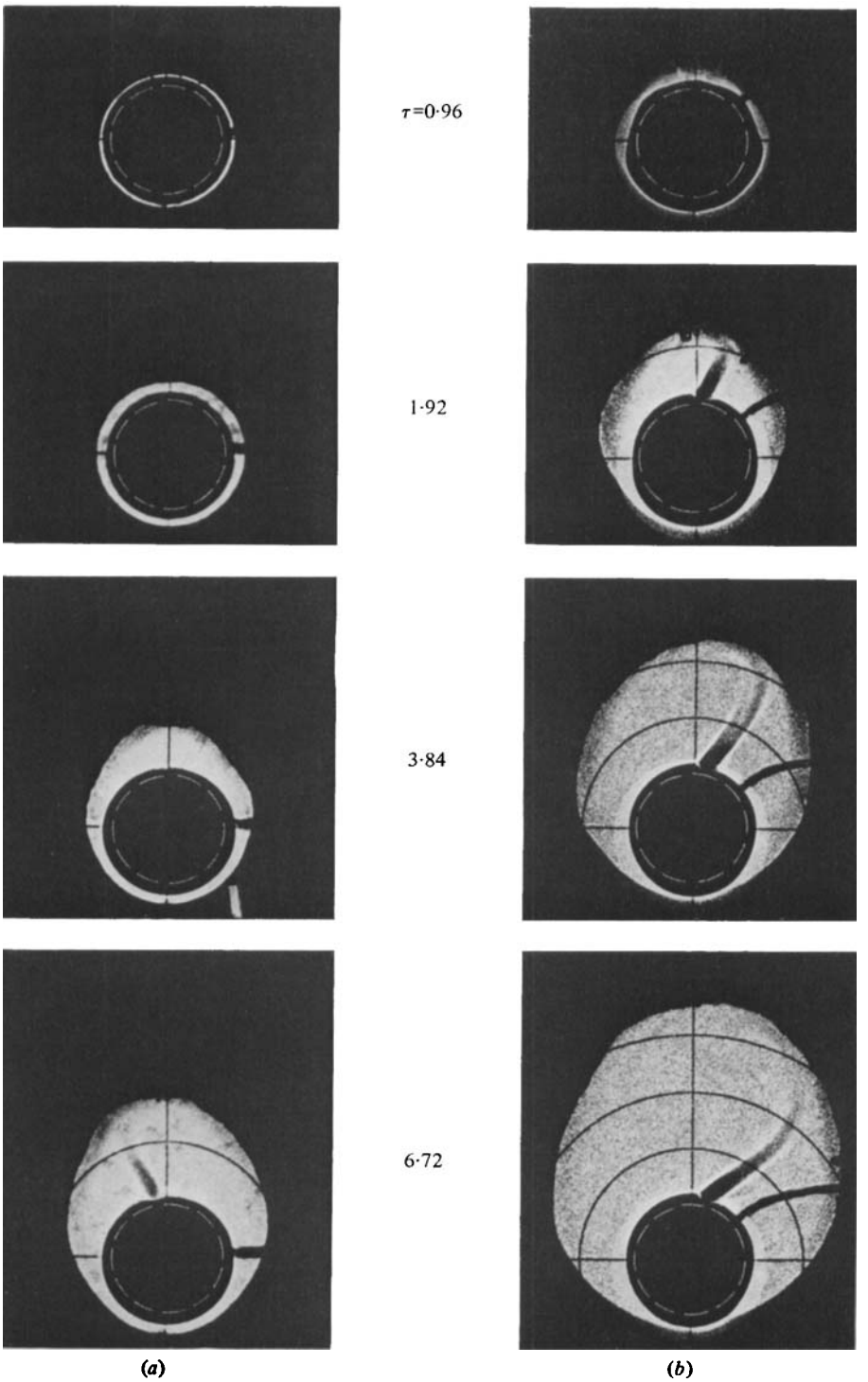

FIGURE 2. Photographs illustrating the position of the solid–liquid interface at different times: (*a*) *Ste* = 0·587 and (*b*) *Ste* = 1·175.

(*a*)

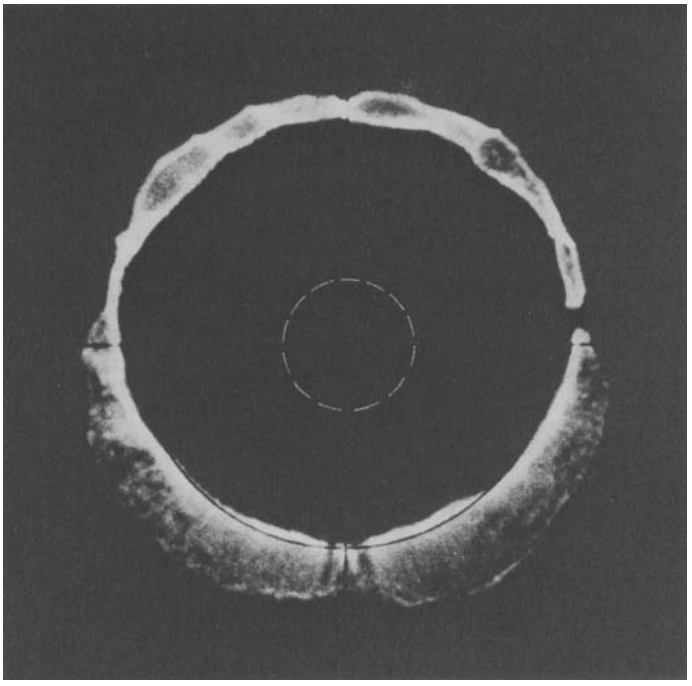

(*b*)

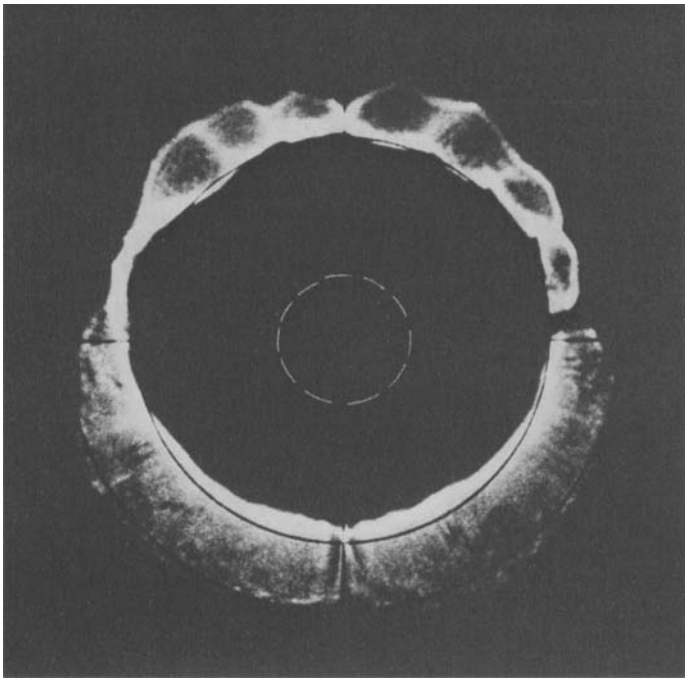

FIGURE 7. Photographs illustrating development of natural convection during the melting process for $Ste = 0{\cdot}587$: (*a*) $\tau = 1{\cdot}92$ and (*b*) $\tau = 2{\cdot}112$.